

# Performance Assessment of Wind Turbines: Data-Derived Quantitative Metrics

Yusen He and Andrew Kusiak, *Member, IEEE*

**Abstract**—Deteriorating performance of wind turbines results in power losses. A two-phase approach for performance evaluation of wind turbines is presented at past and future time intervals. Historical wind turbine data is utilized to determine the past performance, while performance at future time horizons calls for power prediction. In phase I of the proposed approach, wind power is predicted by an ensemble of extreme learning machines using parameters such as wind speed, wind temperature, and the rotor speed. In phase II, the predicted power is used to construct Copula models. It has been demonstrated that the parameters of the Copula models serve as usable metrics for expressing performance of wind turbines. The Frank Copula model performs best among the five parametric models tested.

**Index Terms**—Wind turbine performance evaluation, Performance metrics, Parametric Copula models, Extreme learning machine, Linear ensemble, Tail dependence analysis

## I. INTRODUCTION

The operations and maintenance (O&M) activities of wind turbines impact profitability of wind power generation [1-8]. The O&M cost is closely correlated to the performance of wind turbines. Deteriorating performance of a wind turbine may be caused by the failing components of the power train, converter, or the yaw mechanism [9]. Failure of these components and assemblies impacts the turbine maintenance cost [10-11]. Factors such as variations of the wind speed and air density may also impair performance of a wind turbine.

Performance of any system is usually expressed by a ratio of the system output and the input which tends to be linear. Assessing performance of a wind turbine is difficult due to inherent nonlinearity between the input (wind speed) and the output (power generated). It is further complicated by the distribution of faults across the working envelope. There is no usable metric for measuring performance of wind turbines. The literature on performance evaluation of wind turbines has focused on physics-based and data-driven modeling. The physics-based approaches encompass parametric and nonparametric reliability models [12-13]. Fatigue analysis applied to estimation of the lifetime of turbine components has been studied in [14]. Most physics-based models are fault specific and involve probability distributions of faults. The fatigue analysis methods and reliability models are useful in analyzing and predicting faults of specific components. However, wind turbines are complex assemblies and their performance is impacted by different factors. The latter limits the use of physics-based approaches. The data-driven

approaches have been used to model different phenomena in wind turbines, including visualizing performance of wind turbines [15]. Prediction of wind power is key to anticipating changes in performance of wind turbines. Time-series models, such as autoregressive moving average (ARMA) and generalized autoregressive conditional heteroskedasticity (GARCH) have been applied for prediction of wind power output in [16-17]. Serial correlation and seasonality characteristics of wind speed and wind power can be detected by these models. The time-series models are usually less accurate than the machine learning models. Neural network (NN) and fuzzy logic models were developed for predictive modeling of wind power [18-19]. The extreme learning machine (ELM) approach was applied to predict wind power in [20-21]. In comparison to the traditional algorithms such as support vector machines (SVMs) and neural networks (NNs), the ELM algorithm appears to work faster and it provides more accurate predictions. Some studies have focused on evaluating turbine performance with statistical approaches. Gill and Stephen [22] applied empirical Copula models for early recognition and anticipation of degradation of blades, yaw mechanism, and the pitch system. Based on their research, Wang and Infield [23] applied a mixed Gaussian parametric Copula model for performance evaluation of wind turbines.

In this research, ELM-Copula modeling is applied to express performance of wind turbines. A linear ensemble of ELMs based on LASSO (least absolute shrinkage and selection operator) regularization [24] predicts wind power. Traditional machine learning models such as NN, SVM, and ELM are suitable for short-horizon predictions, however, they provide less accurate results for longer prediction horizons. With the LASSO regularization [25], the proposed ensemble approach provides more accurate results than any independent ELM. To quantify turbine performance, tail dependency and concordance measurement metrics are applied in this paper. For tail dependency analysis, parametric Copula models are used to test the measured wind speed and predicted wind power. The maximum likelihood estimation is used for the parameters of the Copula models. Two concordance measurement metrics, Kendall's tau and Spearman's rho, are computed using the estimated parameters to evaluate turbine performance. The benefits of the proposed approach, including the tau and rho metrics, are demonstrated with computational experiments.

## II. DATA-DRIVEN METHODOLOGY

The power generated by a turbine is impacted by the variable wind conditions, air density, and component

malfunctions [9]. For example, gearbox faults and pitch misalignment lead to power losses visible in a power curve. The decreased performance of a wind turbine is indicated by points outside the contour of the power curve. A well-performing wind turbine has fewer points scattered outside of the dominant power curve contour. Visual analysis of power curves based on historical data is inaccurate, and impossible at future time horizons.

In this paper, a methodology utilizing extreme learning machine (ELM) and Copula models is proposed to analyze tail dependence and concordance between the measured wind speed and the predicted wind power. The dataset used in the study has been collected from an operating wind farm in the period January 2013 to December 2015. The data collected feeds the modeling framework presented in Fig. 1. The daily average wind data from 2013 and 2014 is utilized for training and the data of 2015 is utilized for model validation.

The SCADA data is preprocessed with imputation of missing values and removal of redundancies. In phase I of the methodology in Fig. 1, parameters are selected by the Relief-F algorithm [26-27]. The wind speed is used to predict the wind power by the MLE-ELM approach. In phase II, the marginalized distributions of the measured wind speed and predicted wind power are constructed. Five parametric Copula models are fitted and parameters of each model are derived by the maximum likelihood estimation (MLE). The performance of parametric Copula models is evaluated with the Akaike information criterion (AIC) and the Bayesian information criterion (BIC). Copula models with the smallest values of AIC and BIC perform best.

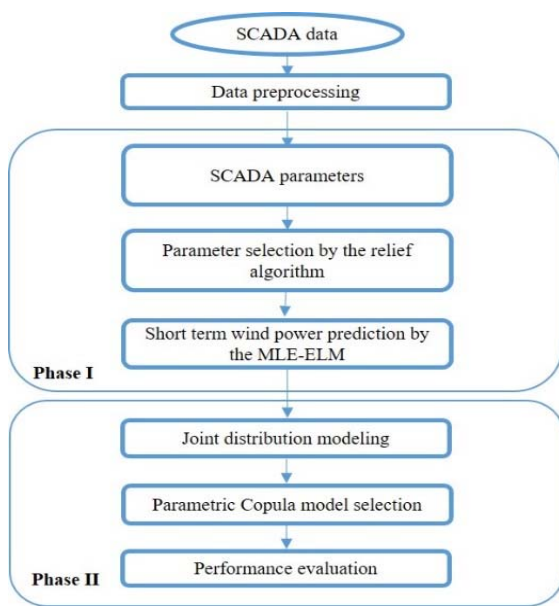


Fig. 1. The data-driven modeling framework.

#### A. Extreme Learning Machine

Traditional machine learning algorithms such as naïve Bayes and zero R can be not accurate. Support vector machines (SVMs) are more promising in classification on high-dimensional data [28]. However, the performance of SVM in regression depends on the kernel functions selected. A multiple linear perceptron (MLP) algorithm usually performs well,

however, overfitting and expensive training are commonly reported. Extreme learning machine (ELM) overcomes these drawbacks and it has proven to offer good prediction accuracy across many applications [29-31].

The basic ELM algorithm consists of three layers: input layer, hidden layer, and output layer. Given the training set  $(x_i, t_i)$ , the hidden node output function  $G(a, b, x)$ , and the number of hidden nodes  $L$ , the learning model is expressed in (1)-(2).

$$f_L(x_j) = o_j, \forall j \quad (1)$$

$$\sum_{i=1}^L \beta_i G(a_i, b_i, x_j) = t_j, j = 1, 2, \dots, N \quad (2)$$

where:  $x_j$  represents the input parameters;  $o_j$  represents the predicted output values;  $f_L()$  is the non-linear function representing the ELM algorithm;  $a_i$  is the weight vector connecting the  $i^{th}$  hidden node and the input nodes;  $b_i$  is the threshold of the  $i^{th}$  hidden node;  $\beta_i$  is the weight vector connecting the  $i^{th}$  hidden node and the output nodes; and  $t_j$  is the actual output value. To evaluate the performance of ELM, the two following metrics are used: the RMSE (root mean square error (3)) and the MAPE (mean absolute percentage error) (4).

The extreme learning machine (ELM) is stated next [32]:

**Step 1:** Hidden node parameters  $a_i$  and  $b_i$  are randomly assigned.

**Step 2:** The hidden layer output matrix  $H$  is computed from (5).

**Step 3:** The output weight  $\beta$  is computed as  $\beta = H^+ T$ , where  $H^+$  is the Moore-Penrose generalized inverse of hidden layer output matrix  $H$ .

$$\text{RMSE} = \sqrt{\frac{1}{N} \sum_{j=1}^N \|o_j - t_j\|^2} \quad (3)$$

$$\text{MAPE} = \frac{1}{N} \sum_{i=1}^n \left| \frac{o_i - t_i}{t_i} \right| \quad (4)$$

$$H = \begin{bmatrix} G(a_1, b_1, x_1) & \dots & G(a_L, b_L, x_1) \\ \vdots & \ddots & \vdots \\ G(a_1, b_1, x_N) & \dots & G(a_L, b_L, x_N) \end{bmatrix}_{N \times L} \quad (5)$$

#### B. A Linear Ensemble of Extreme Learning Machines (ELM) based on LASSO Regularization

The basic extreme learning algorithm randomly assigns hidden nodes and incrementally updates the output weights of the hidden layer nodes. However, finding the optimal number of hidden nodes minimizing the training error is a challenge. A number of algorithms has been proposed to minimize the training error and offer satisfactory generalization capability. For example, improved prediction accuracy has been reported with the bidirectional extreme learning machine (B-ELM), online-sequential extreme learning machine (OS-ELM), and multilayer hierarchical extreme learning machine (H-ELM). In this paper, a LASSO (least absolute shrinkage and selection operator) regularized linear ensemble of ELMs (MLE-ELM) is employed to predict wind power.

Yu [33] proposed a double-regularized extreme learning machine (ELM) with LASSO regularization and Tikhonov regularization. In this paper, the LASSO regularization is

selected as the ensemble method of ELMs. The LASSO regularization is expressed in (6).

$$\min_{\lambda, \omega} \left( \sum_{i=1}^N (y_i - x_i \omega)^2 + \lambda \sum_{j=1}^P |\omega_j| \right) \quad (6)$$

where:  $x_i$  denotes the input parameter;  $y_i$  represents the measured output value;  $\omega$  is the regression weight; and  $\lambda$  is the non-negative regularization parameter. The aim of LASSO regularization is to optimize the output by changing the output weights of the multiple ELMs.

### C. Copula-based Joint Distribution Modeling

The most direct indication of underperformance of a wind turbine is in the abnormal tail dependency and co-movement between the measured wind speed and the predicted wind power. Co-movement is the correlated movement of wind speed and wind power [38]. Tail dependence expresses the propensity of the wind speed and wind power jointly moving up and down [36]. To investigate the dependence and co-movement, parametric Copula models are constructed. The Copula model was originally proposed by Sklar [34-35] as an  $N$ -dimensional joint distribution function expressed as a composition of  $N$  univariate marginal distribution functions and a suitable Copula function. To evaluate performance of a wind turbine, two marginal distributions of the measured wind speed and the predicted wind power are established. The general Copula model is expressed in (7).

$$F(x_1(t), x_2(t)) = C[F_{x_1}(x_1(t)), F_{x_2}(x_2(t))] \quad (7)$$

where:  $x_1$  is the measured wind speed; and  $x_2$  represents the predicted wind power;  $F(x_1)$  and  $F(x_2)$  are the marginal cumulative density functions (CDFs) of the measured wind speed and the predicted wind power;  $F(x_1, x_2)$  is the two-dimensional joint distribution; and  $C(u_1, u_2)$  is the Copula function.

The Copula modeling of wind turbine performance offers several advantages. First, the Copula approach captures the marginal behavior of measured wind speed and predicted wind power. The dependence structure between these two parameters is established. The degree of dependence and the dependence structure are expressed with a Copula function [36]. In addition, Copula models capture the tail dependence and measure the co-movement.

### D. Parametric Copula Models

Among several parametric Copula models, two Copula families, the Elliptical Copula and Archimedean Copula family are frequently used. The Elliptical Copula family includes Gaussian Copula and Student-t Copula. The Archimedean Copula family includes Gumbel Copula, Clayton Copula, and Frank Copula. As illustrated in Table I, among Archimedean Copulas, only the Gumbel Copula model reflects the upper tail dependence with high sensitivity. The Clayton Copula is suitable for modeling the lower tail dependence. For Elliptical families, both Student-t Copula and Gaussian Copula model are symmetric. Student-t Copula models both lower tail and upper tail dependence. The Frank Copula model evaluates concordance between two highly associated variables with

heavily-tailed distributions. The Gaussian Copula does not model tail dependence.

TABLE I.  
SUMMARY OF COPULA MODELS

Copula	Archimedean Copula	Extreme Value Copula	Lower Tail Dependence	Upper Tail Dependence
Gaussian	No	No	No	No
Student-t	No	No	Yes	Yes
Gumbel	Yes	Yes	No	Yes
Clayton	Yes	No	Yes	No
Frank	Yes	No	No	No

The preliminary analysis of the measured wind speed and the predicted wind power indicates that their marginal distribution is right fat-tailed. Hence, the Archimedean Copula is selected for modeling. The model performance is assessed with the Akaike information criterion (AIC) and Bayesian information criterion (BIC) presented in (8) and (9), respectively.

$$AIC = 2k - 2\ln(L) \quad (8)$$

$$BIC = -2\ln(L) + k * \ln(n) \quad (9)$$

where:  $k$  denotes the number of estimated parameters;  $L$  denotes the maximum value of the likelihood function; and  $n$  represents the total number of samples used in the model development.

In this study, the Spearman's rho (10) and Kendall's tau (11) concordance metrics are computed to detect co-movement anomalies.

$$\tau_{Frank} = 1 + \frac{4[D_1(\alpha) - 1]}{\alpha} \quad (10)$$

$$\rho_{Frank} = 1 + \frac{12[D_2(\alpha) - D_1(\alpha)]}{\alpha} \quad (11)$$

where:  $D_m(x)$  is the first order of Debye function [37] defined in (12).

$$D_m(x) = \frac{m}{x^m} \int_0^x \frac{t^m}{e^t - 1} dt \quad (12)$$

## III. CASE STUDY

In this section the proposed approach is illustrated with a case study. The 10-min wind farm data collected from Jan 1<sup>st</sup> 2013 to Dec 31<sup>st</sup> 2014 was used to construct the ELM-Copula model and assess turbine performance. One year data collected from Jan 1<sup>st</sup> to Dec 31<sup>st</sup> in the year of 2015 was selected to validate the constructed model.

The SCADA summarized in Table II has been partitioned into 1095 files based on the fixed time interval. Each file contains a day of data.

### A. Parameter Selection with the Relief-F Algorithm

The dataset used in this case study includes 26 parameters, e.g., wind speed, rotor speed, temperature, averaged over 10 min intervals.

TABLE II.  
DATASET DESCRIPTION

Dataset	Number of Records	Time Period
Total set	157825	1/1/2013-12/31/2015
Training set	105121	1/1/2013-12/31/2014
Test set	52704	1/1/2015-12/31/2015

To determine relevancy of each parameter, the relief-F algorithm is applied. It is an instance-based unsupervised learning heuristic algorithm that identifies parameters that are relevant to the target output [26]. It overcomes a deficiency of

the original relief algorithm of coping with the nearest neighbors that are not well defined in the weighted feature space. By averaging  $k$  nearest neighbors when computing sample margins, significant performance improvement has been reported [27].

Table III demonstrates performance of the candidate parameters for different values of  $k$ . The average rotor speed, wind speed, and wind temperature have high relevancy to the wind power. Hence, three input parameters, the average rotor speed, wind speed, and wind temperature are selected to predict wind power.

TABLE III.  
PARAMETER SELECTION BY THE RELIEF-F ALGORITHM

k	Wind speed	Wind temperature	Rotor speed	Gear oil temperature	Ambient temperature	Working hours	Hours without grid	Alarm frequency	Break released	Generator cut-in	Status code	Set point	Alarm frequency
10	0.049	0.017	0.015	0.005	0.003	0.000	0.000	0.001	0.001	0.001	0.001	0.005	0.005
15	0.056	0.023	0.013	0.005	0.002	0.000	0.000	0.001	0.002	0.001	0.001	0.004	0.006
20	0.060	0.026	0.012	0.005	0.001	0.002	0.003	0.000	0.004	0.001	0.000	0.003	0.007
25	0.064	0.028	0.011	0.006	0.000	0.001	0.001	0.001	0.003	0.001	0.001	0.002	0.009
30	0.067	0.031	0.009	0.005	0.000	0.000	0.000	0.001	0.002	0.001	0.001	0.002	0.010

### B. The LASSO Regularized Linear Ensemble of Extreme Learning Machines

The historical wind data from the year 2013 and 2014 is utilized to develop an extreme learning machine (ELM) model. The daily average and daily standard deviation of the historical wind power are computed. Performance of the extreme learning machine algorithm is compared with the support vector machine (SVM), multi-layer perceptron (MLP), basic extreme learning machine (ELM), bidirectional extreme learning machine (B-ELM), online sequential extreme learning machine (OS-ELM), and least absolute shrinkage and selection operator

(LASSO) regularized linear ensemble of extreme learning machines (MLE-ELM) models.

Table IV illustrates prediction performance of the seven models expressed in two metrics, RMSE (4) and MAPE (5).

The MLE-ELM model produces the smallest RMSE and MAPE values. The testing performance of the MLE-ELM predicting the wind power for the year of 2015 is illustrated in Fig. 2.

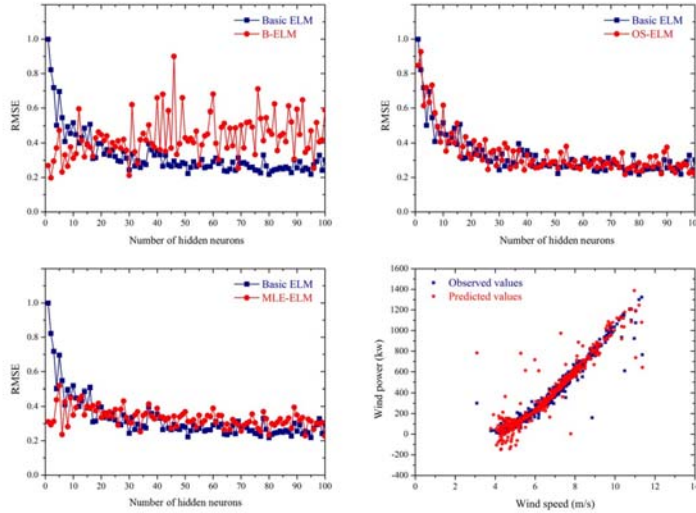


Fig. 2. Performance comparison of two models.

TABLE IV.  
PERFORMANCE EVALUATION OF SEVEN MODELS

Algorithm	SVM	MLP	ELM	B-ELM	H-ELM	OS-ELM	MLE-ELM
RMSE	0.488	0.441	0.447	0.452	0.722	0.532	<b>0.436</b>
MAPE (%)	6.315	4.574	4.262	4.365	9.637	8.773	<b>4.155</b>

RMSE is the root mean square error; MAPE is the mean average percentage error.

### C. Joint Distribution Analysis of Measured Wind Speed and Predicted Wind Power

Performance of wind turbines is evaluated with Copula models of the measured wind speed and predicted wind power. There are two major approaches to Copula modeling, parametric and non-parametric. The non-parametric empirical Copula models evaluate the average dependency and concordance based on the empirical distribution with a smooth kernel. The parametric approach models the tail dependence and the co-movement from data. The deteriorating performance may be reflected by anomalies in the tail dependence and co-movement. Hence, the parametric Copula models are constructed for turbine performance evaluation. Table V offers summary of four basic statistics of the measured wind speed and the predicted power in three years. Skewness is the third central moment of the mean and it measures the asymmetry. Kurtosis is the fourth central moment of the mean and it measures the heavy tails.

TABLE V.  
STATISTICS OF THE MEASURED WIND SPEED AND THE PREDICTED WIND POWER

Year	Parameter	Mean	SD	Skewness	Kurtosis
2013	Wind speed (m/s)	8.48	0.77	-0.8	-0.55
	Wind power (kW)	759.7	166.85	0.75	-0.66
2014	Wind speed (m/s)	8.58	1.09	0.17	-0.82
	Wind power (kW)	764.76	215.18	0.32	-1.07
2015	Wind speed (m/s)	8.42	0.86	-0.7	-0.99
	Wind power (kW)	741.12	176.82	0.73	-1.11

In 2015, the average measured wind speed was 8.42 m/s and its predicted mean wind power was 741.12 kW. The

negative value of skewness in 2015 of average measured wind speed indicates a low probability of wind speed exceeding the average measured wind speed. The positive skewness value of the predicted wind power in 2015 points to a higher chance of wind power exceeding the predicted mean wind power. A satisfactory performance in 2015 can be expressed by the skewness of both average measured wind speed and predicted mean wind power. In 2014 the average measured wind speed was 8.58 m/s and the predicted mean wind power was 764.76 kW. The positive values of the skewness of the measured wind speed in 2014 suggests a high probability of higher wind speed. However, the skewness of the predicted wind power in 2014 is low. In 2013, the skewness values of both measured wind speed and predicted wind power are almost identical to the ones in 2015. Nevertheless, the kurtosis of the predicted wind power in 2013 is the highest in the three years which indicates more frequent occurrence of extreme power changes. Hence, the two basic statistics indicate improving turbine performance in 2015.

Table VI presents the normality tests results. The normality tests are conducted based on 10 min data from January 2013 to December 2015. The Anderson-Darling (A-D) test, Jarque-Bera (J-B) test, and Lilliefors (LF) test have been applied to test the normality of the measured wind speed and predicted wind power over the three years. The A-D test stat denotes the  $A$  statistics of the normality test. The J-B test stat is the  $\chi^2$  statistic of the normality test. The LF test stat is the Kolmogorov-Smirnov Goodness-of-Fit test statistic of the normality test. Since all p-values are lower than 0.05, the normality of the marginal distributions of the measured wind speed and the predicted wind power is rejected. The computational results has validated the wind energy experience.

TABLE VI.  
NORMALITY TEST RESULTS

Dataset	Parameter	A-D Test		J-B Test		LF Test	
		Test Stat	p-Value	Test Stat	p-Value	Test Stat	p-Value
2013	Wind speed (m/s)	281.754	0.0005	2918.4	0.0010	0.0564	0.0010
	Wind power (kW)	840.619	0.0005	3112.6	0.0010	0.0881	0.0010
2014	Wind speed (m/s)	350.565	0.0005	2957.8	0.0010	0.0643	0.0010
	Wind power (kW)	947.466	0.0005	3135.3	0.0010	0.0920	0.0010
2015	Wind speed (m/s)	361.668	0.0005	2958.7	0.0011	0.0684	0.0011
	Wind power (kW)	954.164	0.0005	3216.1	0.0011	0.0982	0.0010

### D. Co-movement Analysis with Parametric Copula Modeling

Table VII illustrates parameters of the Copula models of the measured wind speed and the predicted wind power. Using the two year SCADA data, Copula parameters of the Elliptical and Archimedean Copula families are estimated by the

maximum likelihood estimation (MLE). The Akaike information criterion (AIC) and the Bayesian information criterion (BIC) are computed. The AIC and BIC are defined in Section 2.4 (see expressions (8)-(9)). The smaller values of AIC and BIC indicate better performance of the parametric Copula model.

The small value (between 2 and 5) of the degree of freedom of the Student-t Copula models suggests a substantial co-movement and tail dependence. The AIC values of Student-t Copula models are smaller than those of the Gaussian Copula models. This indicates a rejection of the symmetric no-tail dependence structure implied by the Gaussian Copulas [36]. For Archimedean Copula models, the estimated parameters of the Clayton Copula and the Gumbel Copula suggest a statistically significant level of upper tail dependence and lower tail dependence. The computed values of the Clayton Copula parameter are 2.66, 2.69, and 2.84 for 2013, 2014, and 2015 wind data, respectively. For the Gumbel Copula model, the upper tail dependence values are 1.60, 1.48, and 1.62 for 2013, 2014, and 2015 wind data, respectively. These dynamic values indicate deteriorating performance of a wind turbine in 2014 expressed by a significant decrease in the values of the upper tail dependence.

TABLE VII. PARAMETER ESTIMATION OF COPULA MODELS			
Dataset	2013	2014	2015
<b>Elliptical Family</b>			
Gaussian Copula			
$\rho$	0.93	0.92	0.94
Loglikelihood	-13314.40	-13508.00	-13785.50
AIC	-26627.10	-27015.50	-27570.60
BIC	-26620.90	-27016.40	-27571.10
Student-t Copula			
$\rho$	0.70	0.66	0.72
$v$	4.89	4.72	3.86
-Loglikelihood	-13966.00	-11671.20	-14642.60
AIC	-27391.10	-23341.00	-29283.60
BIC	-27374.40	-23324.50	-29265.40
Archimedean Family			
Clayton Copula			
$\alpha$	2.66	2.69	2.84
Loglikelihood	-13468.25	-12450.85	-14361.00
AIC	-26934.20	-24899.60	-28720.50
BIC	-26925.00	-24890.00	-28711.00
Gumbel Copula			
$\delta$	1.60	1.48	1.62
Loglikelihood	-6650.40	-5020.10	-7066.10
AIC	-13299.00	-10038.40	-14131.00
BIC	-13291.20	-10029.60	-14123.50
Frank Copula			
$\theta$	5.61	5.44	5.90
Loglikelihood	-18181.00	-17198.10	-19076.50
AIC	-36360.20	-34395.00	-38150.00
BIC	-36351.40	-34387.20	-38142.20

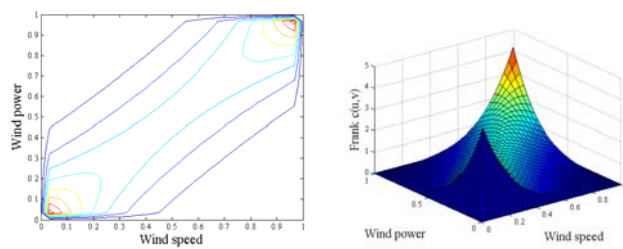


Fig. 3. Contour plot and dependency structure of the fitted Frank Copula model.

Performance of the parametric Copula models is summarized in Table VII. All Copula parameters are estimated by the maximum likelihood estimator (MLE). The Akaike information criteria (AIC) and Bayesian information criteria (BIC) values are computed to assess performance of the Copula models. In comparison with the Elliptical Copula models which are symmetric, the Archimedean Copula models performs better. The average AIC and BIC values of the Archimedean Copulas are smaller than those of the Elliptical. The Frank Copula model has produced the minimum values of AIC and BIC and hence it is selected to measure the co-movement. The joint distribution of the measured wind speed and the predicted wind power fitted by the Frank Copula model is shown in Fig. 3.

The Spearman's rho and Kendall's tau are concordance measurement metrics of parametric Copula models. The positive tau and rho values indicate the measured wind speed and the predicted wind power co-move in the same direction. The Kendall's tau metric indicates that the probability of concordance is significantly higher than the probability of discordance between the measured wind speed and the predicted wind power. A positive value of Spearman's rho indicates correlation between the measured wind speed and the predicted wind power [36].

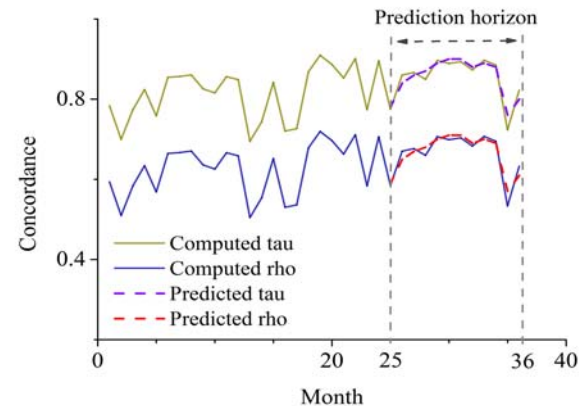


Fig. 4. Monthly tau and rho concordance measurement metrics.

The computed and the predicted values of Kendall's tau and Spearman's rho metrics are illustrated in Fig. 4 at a monthly resolution. The training data is collected from January 2013 through December 2014 (2 year data). The prediction horizon spans over January 2015 through December 2015. In the first two years, the turbine performance is variable. In the summer and fall seasons, the turbine is usually well-performing (high values of tau and rho). The lower values of tau and rho began to emerge in winter and early spring which indicate degrading turbine performance. In the 13<sup>th</sup> month, the predicted value of tau and rho point to underperformance. The lower performance in the winter of 2013, 2014, and 2015 indicates maintenance shortcomings.

#### E. Model Validation with Wind Power Curves and Energy Loss

To evaluate robustness of the data-driven approach, power curves at monthly intervals have been established. Fig. 5 illustrates monthly power curves at different performance

levels: well performing, moderately performing, and underperforming. According to Fig. 4, the best performance occurs in the summer and fall seasons. In September 2015, the value of tau is 0.91 and the rho value is 0.72, both above the average. The corresponding power curve in Fig. 5(a) illustrates the well performing scenario with all data points located around the power curve contour. For the moderate performance scenario illustrated in Fig. 5(b), tau is 0.8 while rho is 0.61. A larger number of points scattered outside the power curve contour is indicative of low turbine performance. The lowest performance occurred in the 13<sup>th</sup> month (January 2014), with tau of 0.69 and rho of 0.48. This scenario is illustrated in Fig. 5(c) where a large number of outliers is observed.

To further validate the model, Pearson's correlation coefficient between the monthly energy loss and tau and rho in years 2013, 2014, and 2015 has been computed (see Table VIII). The correlation coefficient for the data in Fig. 6 varies between -0.88 and -0.89 which demonstrates negative linear correlation between the energy loss tau and rho. For example, the energy loss is 0 kWh, 3510.93 kWh, and 8009.02 kWh in September 2015, January 2013, and January 2014, respectively. The correlation analysis has confirmed that small values of tau and rho indicate higher energy loss and thus point to lower turbine performance.

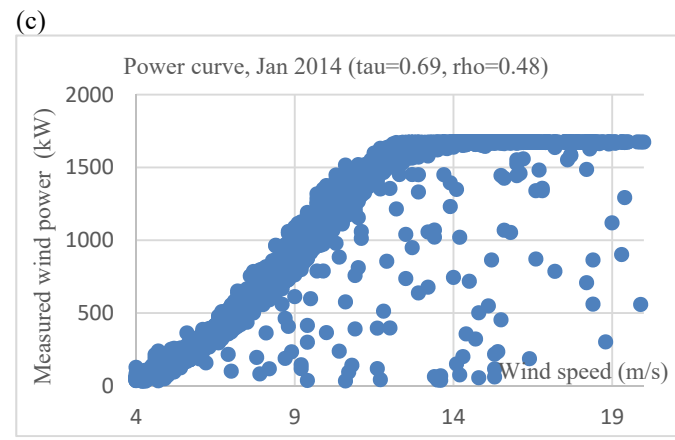
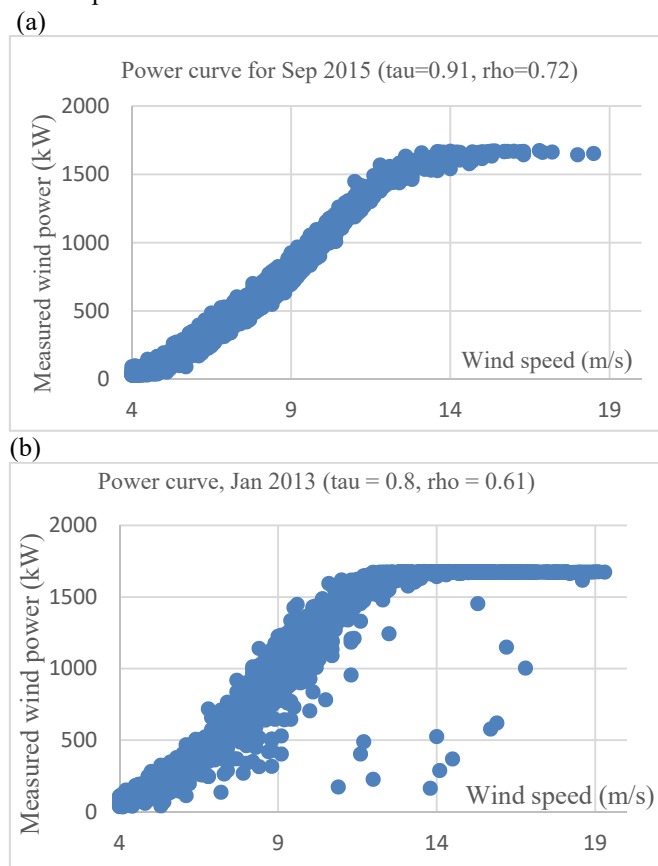


Fig. 5. Monthly power curves for different performance levels.

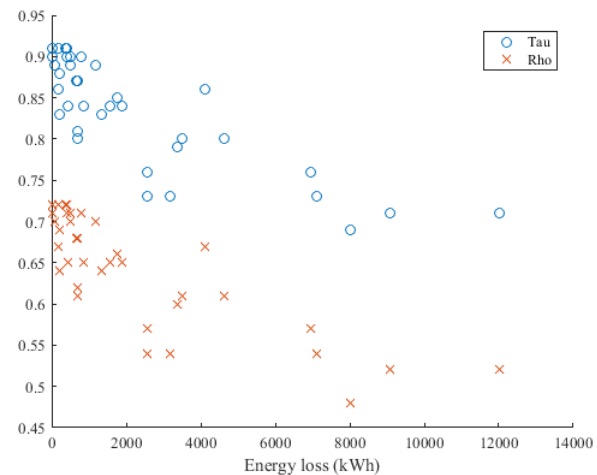


Fig. 6. Relationship between tau, rho, and energy loss.

#### IV. CONCLUSION

In this paper, a data-driven approach for performance evaluation of wind turbines at the past and future time intervals was developed. An ensemble of extreme learning machine was applied to develop models to predict wind power needed for turbine performance assessment at future time horizons. Industrial data collected from of a wind farm was utilized to train and validate the developed ensemble of extreme learning machines.

The developed prediction models were integrated with the parametric Copula models. The parameters of the Copula models provided metrics for performance assessment of wind turbines. Among the five parametric Copula models studied, the Frank Copula model performed best. The model performance was measured with Kendall's tau and Spearman's rho metrics.

Computational results reported in the paper have confirmed validity of the tau and rho metrics in performance evaluation of wind turbines. In the future research, other parametric Copula models such as time-series Copulas (e.g., vine Copula) and multivariate Copulas (e.g., factor Copula) will be studied to explore different aspects of turbine performance. Multivariate dependency and time varying parameterization will be considered to develop more accurate models.

## REFERENCES

- [1] E. Hau, *Wind Turbines*, 2013, Springer, NY, pp. 789-843.
- [2] A. Kusiak, Z. Zhang, and A. Verma, Prediction, operations, and condition monitoring in wind energy. *Energy*, 2013, 60, pp.1-12.
- [3] D. B. Nelson, M. H. Nehrir, and C. Wang, Unit sizing and cost analysis of stand-alone hybrid wind/PV/fuel cell power generation systems. *Renewable Energy*, 2006, 31(10), pp.1641-1656.
- [4] C. A. Walford, Wind turbine reliability: Understanding and minimizing wind turbine operation and maintenance costs. *Sandia National Laboratories Report SAND2006-1100*, 2006, pp. 1-26.
- [5] G. M. J. Herbert, S. Iniyian, E. Sreevalsan, and S. Rajapandian, A review of wind energy technologies. *Renewable and Sustainable Energy Reviews*, 2007, 11(6), pp.1117-1145.
- [6] A. Kusiak, W. Li, and Z. Song, Dynamic control of wind turbines. *Renewable Energy*, 2010, 35(2), pp. 456-463.
- [7] S. A. Huyer, D. Simms, and M. C. Robinson, Unsteady aerodynamics associated with a horizontal-axis wind turbine. *AAAI Journal*, 1996, 34(7), pp. 1410-1419.
- [8] R. W. Hyers, J. G. McGowan, K. L. Sullivan, J. F. Manwell, and B. C. Syrett, Condition monitoring and prognosis of utility scale wind turbines. *Energy Materials*, 2006, 1(3), pp. 187-203.
- [9] F. Spinato, P. J. Tavner, G. J. W. Van Bussel, and E. Koutoulakos, Reliability of wind turbine subassemblies. *Renewable Power Generation*, 2009, 3(4), pp. 387-401.
- [10] P. Tavner, R. Li., and J. Penman, *Condition Monitoring of Rotating Electrical Machines*. IERT Power and Energy Series, 56. IET, London, UK, 2008.
- [11] A. Kusiak and A. Verma, A data-driven approach for monitoring blade pitch faults in wind turbines. *IEEE Transactions on Sustainable Energy*, 2011, 2(1), pp. 87-96.
- [12] C. C. Chen, J. R. Lee, and H. J. Bang, Structural health monitoring for a wind turbine system: a review of damage detection methods. *Measurement Science and Technology*, 2008, 19(12), pp. 122-123.
- [13] C. S. Gray and S. J. Watson. Physics of failure approach to wind turbine condition based maintenance. *Wind Energy*, 2010, 13(5), pp. 395-405.
- [14] L. Rodriguez, E. Garcia, F. Morant, A. Correcher, and E. Quiles. Application of latent nestling method using coloured petri nets for the fault diagnosis in the wind turbine subsets. *IEEE International Conference on Emerging Technologies and Factory Automation*, 2008, pp. 767-773.
- [15] B. Stephen, S.J. Galloway, D. McMillan, D.C. Hill, and D.G. Infield, A copula model of wind turbine performance. *IEEE Transactions on Power Systems*, 2011, 26(2), pp. 965-966.
- [16] F. H. M. El-Fouly, F. Saadany, and M. Salama, One day ahead prediction of wind speed and direction. *IEEE Transactions on Energy Conversion*, 2008, 23(1), pp. 191-201.
- [17] T. Bollerslev, Generalized autoregressive conditional heteroskedasticity. *Journal of Econometrics*, 1986, 31(3), pp. 307-327.
- [18] G. N. Kariniotakis, G. S. Stavrakakis, and E. F. Nogaret, Wind power forecasting using advanced neural networks models. *IEEE Transactions on Energy Conversion*, 1996, 11(4), pp. 762-767.
- [19] C. W. Potter and M. Negnevitsky, Very short-term wind forecasting for Tasmanian power generation. *IEEE Transactions on Power Systems*, 2006, 21(2), pp. 965-972.
- [20] C. Wan, Z. Xu, P. Pinson, Y. D. Zhao, and K. P. Wong, Probabilistic forecasting of wind power generation using extreme learning machine. *IEEE Transactions on Power Systems*, 2014, 29(3), pp. 1033-1044.
- [21] S. Shamshirband, K. Mohammadi, W. T. Chong, D. Petković, E. Porcu, A. Mostafaeipour, S. Ch, and A. Sedaghat, Application of extreme learning machine for estimation of wind speed distribution. *Climate Dynamics*, 2015, 46(5-6), pp. 1893-1907.
- [22] S. Gill, B. Stephen, and S. Galloway, Wind turbine condition assessment through power curve copula modeling. *IEEE Transactions on Sustainable Energy*, 2012, 3(1), pp. 94-101.
- [23] Y. Wang, D. G. Infield, B. Stephen, and S. J. Galloway, Copula-based model for wind turbine power curve outlier rejection. *Wind Energy*, 2014, 17(11), pp. 1677-1688.
- [24] Q. Yu, Y. Miche, E. Eirola, M. Van Heeswijk, E. Severin, and A. Lendasse, Regularized extreme learning machine for regression with missing data. *Neurocomputing*, 2013, 102, pp. 45-51.
- [25] R. Tibshirani, Regression shrinkage and selection via lasso. *Journal of the Royal Statistical Society, Series B*, 1996, pp. 267-288.
- [26] M. Robnik-Sikonja and I. Kononenko, Theoretical and empirical analysis of ReliefF and RReliefF. *Machine Learning*, 2003, 53(1-2), pp. 23-69.
- [27] Y. Sun, Iterative Relief for feature weighting: algorithms, theories, and applications. *IEEE Transactions on Pattern Analysis and Machine Intelligence*, 2007, 29(6), pp. 1035-1051.
- [28] C. J. Burges, A tutorial on support vector machines for pattern recognition. *Data Mining and Knowledge Discovery*, 1998, 2(2), pp.121-167.
- [29] R. Singh and S. Balasundaram, Application of extreme learning machine method for time series analysis. *International Journal of Intelligent Technology*, 2007, 2(4), pp. 256-262.
- [30] N. Y. Liang, P. Saratchandran, G. B. Huang, and N. Sundararajan, Classification of mental tasks from EEG signals using extreme learning machine. *International Journal of Neural Systems*, 2006, 16(1), pp. 29-38.
- [31] Z. L. Sun, T. M. Choi, K. F. Au, and Y. Yu, Sales forecasting using extreme learning machine with applications in fashion retailing. *Decision Support Systems*, 2008, 46(1), pp. 411-419.
- [32] A. Lendasse, A., A. Akusok, O. Simula, F. Corona, M. van Heeswijk, E. Eirola, and Y. Miche, Extreme learning machine: a robust modeling technique? Yes!. *Advances in Computational Intelligence*, Vol. 7902, Springer, New York, NY, 2013, pp. 17-35.
- [33] Q. Yu, Y. Miche, E. Eirola, M. Van Heeswijk, E. Severin, and A. Lendasse, Regularized extreme learning machine for regression with missing data. *Neurocomputing*, 2013, 102, pp. 45-51.
- [34] A. Sklar, Random variables, distribution functions, and copulas---a personal look backward and forward, in L. Rüschendorf, B. Schweizer, and M. D. Taylor, eds. *Distributions with fixed marginals and related topics*, Vol. 28, Institute of Mathematical Statistics, Hayward, CA, 1996, pp. 1-14.
- [35] M. C. Cario and B. L. Nelson, Modeling and generating random vectors with arbitrary marginal distributions and correlation matrix. Technical Report, Department of Industrial Engineering and Management Sciences, Northwestern University, Evanston, Illinois, 1997.
- [36] J. C. Reboredo, How do crude oil prices co-move?: A Copula approach. *Energy Economics*, 2011, 33(5), pp. 948-955.
- [37] L. Zhang and V.P. Singh, Bivariate rainfall frequency distributions using Archimedean copulas. *Journal of Hydrology*, 2007, 332(1), pp. 93-109.
- [38] L. Vacha, and J. Baruník, Co-movement of energy commodities revisited: Evidence from wavelet coherence analysis. *Energy Economics*, 2012, 34(1), pp. 241-247.